doi.org/10.36721/PJPS.2026.39.10.272.1

Network pharmacology and molecular simulation suggest potential mechanisms of sorafenib-induced HFSR

Li qian Wang[1], Si qi Zhang[2], Ling Guo[2], Ji qi Li[2], Li hong Liu[3] and Gui zhi Zhao[2]*

[1]Logistics Group, Jinzhou Medical University, Jinzhou 121001, China
[2]College of Pharmacy, Jinzhou Medical University, Jinzhou 121001, China
[3]Third Affiliated Hospital of Jinzhou Medical University, Jinzhou 121001, China

Abstract: **Background**: Hand–foot skin reaction (HFSR) is a dose-limiting adverse effect of sorafenib, yet its molecular etiology remains elusive. **Objectives**: This study investigated the potential targets and pathways of sorafenib-induced HFSR using integrated computational methods. **Methods**: Network pharmacology was used to identify overlapping targets between sorafenib and HFSR. After pathway enrichment, hub targets were analyzed via molecular docking and 100-ns molecular dynamics (MD) simulations to assess binding stability. **Results**: Network analysis identified 71 targets, primarily in the MAPK/ERK and PI3K-Akt pathways. EGFR and MAPK1 (ERK2) were identified as key hubs. MD simulations revealed that sorafenib maintains superior structural stability when complexed with EGFR rather than with ERK2. **Conclusion**: Computational evidence suggests that off-target engagement and RTK-MAPK/PI3K dysregulation mediate HFSR. These findings provide a mechanistic basis for mitigating sorafenib-induced toxicity, pending experimental validation.

Keywords: EGFR; HFSR; Molecular dynamics simulation; MAPK1 (ERK2); Network pharmacology; Sorafenib

Submitted on 26-07-2025 – Revised on 24-09-2025 – Accepted on 16-12-2025

INTRODUCTION

Sorafenib, a multikinase inhibitor approved by the U.S. FDA, was the first of its kind to be approved for advanced hepatocellular carcinoma (HCC) treatment. It remained the standard systemic therapy until lenvatinib was approved in 2018 (Qin *et al*., 2024). This drug acts by targeting a variety of kinases, such as Raf-1, B-Raf, VEGFR-2/3, PDGFR-β, Flt-3 and c-KIT, leading to its antiproliferative and antiangiogenic effects (Guo *et al*., 2023). In addition to HCC, sorafenib is also used to treat metastatic renal cell carcinoma (Liu *et al*., 2023).

Despite its clinical efficacy, sorafenib is commonly associated with various side effects, such as diarrhea, fatigue, hypertension and especially HFSR. Although most of these events are mild to moderate, they can significantly impair quality of life and necessitate dose reductions or treatment discontinuation, thus limiting therapeutic outcomes (Li *et al*., 2024, Pang *et al*., 2022, Wei *et al*., 2025). Elucidating the molecular mechanisms of the sorafenib-induced toxicity is critical for optimizing patient management (Adefisan-Adeoye *et al*., 2025, Li *et al*., 2024, Liang *et al*., 2022, Lim *et al*., 2023, Rui *et al*., 2025, Trivedi *et al*., 2023).

Among these adverse effects, HFSR is particularly common and clinically significant. First reported as a dose-limiting toxicity during early-phase clinical trials (Inaba *et al*., 2019, Liang *et al*., 2025, Ochi *et al*., 2021, Panetta *et al*., 2021), HFSR has emerged as a leading cause of treatment interruption (Guo *et al*., 2023, Lee *et al*., 2020, Zhang *et al*., 2024). In HCC patients, it is the most prevalent adverse event, characterized by painful hyperkeratotic lesions on pressure-bearing surfaces, distinct from classical chemotherapy-induced hand–foot syndrome (Baby *et al*., 2025, Chen *et al*., 2021, Kumari *et al*., 2022, Pang *et al*., 2022).

From a pharmacokinetic perspective, sorafenib undergoes extensive metabolism primarily via CYP3A4 and UGT1A9 in the liver and intestine (Cai *et al*., 2024, Franczyk *et al*., 2022). Key metabolites include sorafenib N-oxide (M2), which retains pharmacological activity and constitutes a significant circulating component (Gong *et al*., 2017, Wang *et al*., 2023). Given the complex metabolism and variable bioavailability of sorafenib, both the parent drug and its metabolites may contribute to toxicity profiles such as HFSR (Saigusa *et al*., 2021) (Fig. 1).

In this research, we adopted a combined strategy of network pharmacology, molecular docking and MD simulation to investigate the molecular mechanisms underlying sorafenib-induced HFSR. Our findings highlight two key targets—MAPK1 (ERK2) and EGFR—implicated in the pathogenesis of HFSR through their involvement in MAPK and PI3K-Akt signaling pathways. Comparative docking and simulation studies were conducted to evaluate the binding preferences of sorafenib and its major metabolite M2 toward ERK2 and EGFR, offering mechanistic insight into differential target engagement and toxicity.

MATERIALS AND METHODS

Prediction of sorafenib and metabolite targets

The canonical SMILES of sorafenib and its major

**Corresponding author:* e-mail: zhaoguizhi@jzmu.edu.cn

metabolites were generated using ChemDraw and imported into SwissTargetPrediction and SuperPred to predict potential protein targets (Ahmad Roslan *et al*., 2025, Raju *et al*., 2025). For SwissTargetPrediction, targets with a probability > 0.9 were retained, while for SuperPred, only those with a prediction score ≥ 50% were included. Additionally, the ChEMBL database was queried for experimentally validated targets with confidence scores ≥ 90%.

Collection of HFSR-associated genes

Genes associated with HFSR were retrieved by searching GeneCards (Stelzer *et al*., 2016) using keywords such as "hand–foot skin reaction," "palmar-plantar erythrodysesthesia," "skin toxicity," "acral erythema," and "chemotherapy-induced hand–foot syndrome." Genes with a relevance score ≥ 10 were retained. Similarly, DisGeNET (Piñero *et al*., 2020) was searched using the same terms and genes with a GDA score ≥ 0.01 were collected. Duplicate entries were excluded and gene symbols were standardized according to UniProt (Zaru *et al*., 2023). Overlapping targets between sorafenib-related proteins and HFSR-related genes were identified using the bioinformatics platform (Chen *et al*., 2023, Wang *et al*., 2025).

Protein–protein interaction (PPI) network construction

The overlapping targets were imported into the STRING database (Szklarczyk *et al*., 2025), restricting the search to Homo sapiens and retaining only interactions with the highest confidence (score ≥ 0.9); disconnected nodes were removed. The constructed network was visualized using Cytoscape 3.10.4 (Kumar *et al*., 2022). Hub genes were identified through topological analysis with the cytoHubba plugin (Balasundaram *et al*., 2022).

Enrichment analysis methods

Functional and pathway enrichment analyses were performed using Metascape (Song *et al*., 2025). The analysis integrated multiple authoritative databases, including Gene Ontology (GO) Biological Processes, Molecular Functions, Cellular Components, KEGG Pathways, Reactome, WikiPathways, PID and Canonical Pathways. Statistical significance was determined using the hypergeometric test with Benjamini–Hochberg FDR correction. Enriched terms with adjusted $p < 0.01$ were considered significant.

Construction of the compound–target network

A compound–target interaction network comprising sorafenib, its metabolites and predicted targets was constructed using R v4.5.2. Sankey diagrams and bubble plots were generated to highlight key compounds and central targets.

Molecular docking

Molecular docking was performed using Discovery Studio 2017 (Dassault Systemes, BIOVIA). Crystal structures of target proteins were retrieved from the Protein Data Bank (PDB). Symmetrical chains were removed and proteins were prepared using the prepare protein protocol: polar hydrogens were added, protonation states were assigned at physiological pH (7.4) under the CHARMm force field, missing residues were modeled and all crystallographic water molecules were deleted to emphasize direct ligand–protein interactions. Ligands (sorafenib and co-crystallized reference inhibitors) were processed with the prepare ligands module, generating low-energy 3D conformations via energy minimization under the CHARMm force field. Flexible ligand docking was conducted using CDOCKER. The binding site was defined using PDB site records. The top 10 poses were ranked by –CDOCKER Interaction Energy (kcal/mol), incorporating van der Waals, electrostatic and desolvation contributions. Protocol accuracy was validated by redocking reference inhibitors under identical conditions. For EGFR (PDB: 9QXN; ligand: Sevabertinib), the RMSD was 0.5245 Å; for ERK2 (PDB: 6SLG; ligand: AZD0364), RMSD was 0.7410 Å, confirming reliable pose reproduction.

Molecular dynamics simulation

To assess the dynamic stability of the ligand–protein complexes, MD simulations were performed using GROMACS 2021.4 with the CHARMM36 force field (Wieczór *et al*., 2025). Ligand topology files were created via the CGenFF server (Wieczór *et al*., 2025). Each complex was solvated in a dodecahedral box with TIP3P water molecules and periodic boundary conditions were applied. After system equilibration, a 100 ns production run was carried out.

RESULTS

Potential targets of sorafenib and its metabolites associated with HFSR

A total of 321 putative targets of sorafenib and its metabolites were predicted using SwissTargetPrediction, SuperPred and ChEMBL databases. Concurrently, 806 and 68 HFSR-related genes were retrieved from GeneCards and DisGeNET, respectively. After deduplication, 834 unique HFSR-associated genes were retained. Venn analysis revealed 71 overlapping targets potentially implicated in sorafenib-induced HFSR (Fig. 2). Hypergeometric test confirmed significant enrichment of overlapping targets ($k = 71$; $n = 321$; $K = 834$; $N = 1,084$; $p = 1.13 \times 10^{-28}$; enrichment factor = 4.65).

PPI network construction and core target identification

The 71 overlapping targets were imported into the STRING database (version 12.0; https://string-db.org/), with *Homo sapiens* selected as the organism and a minimum interaction score of 0.9 (highest confidence).

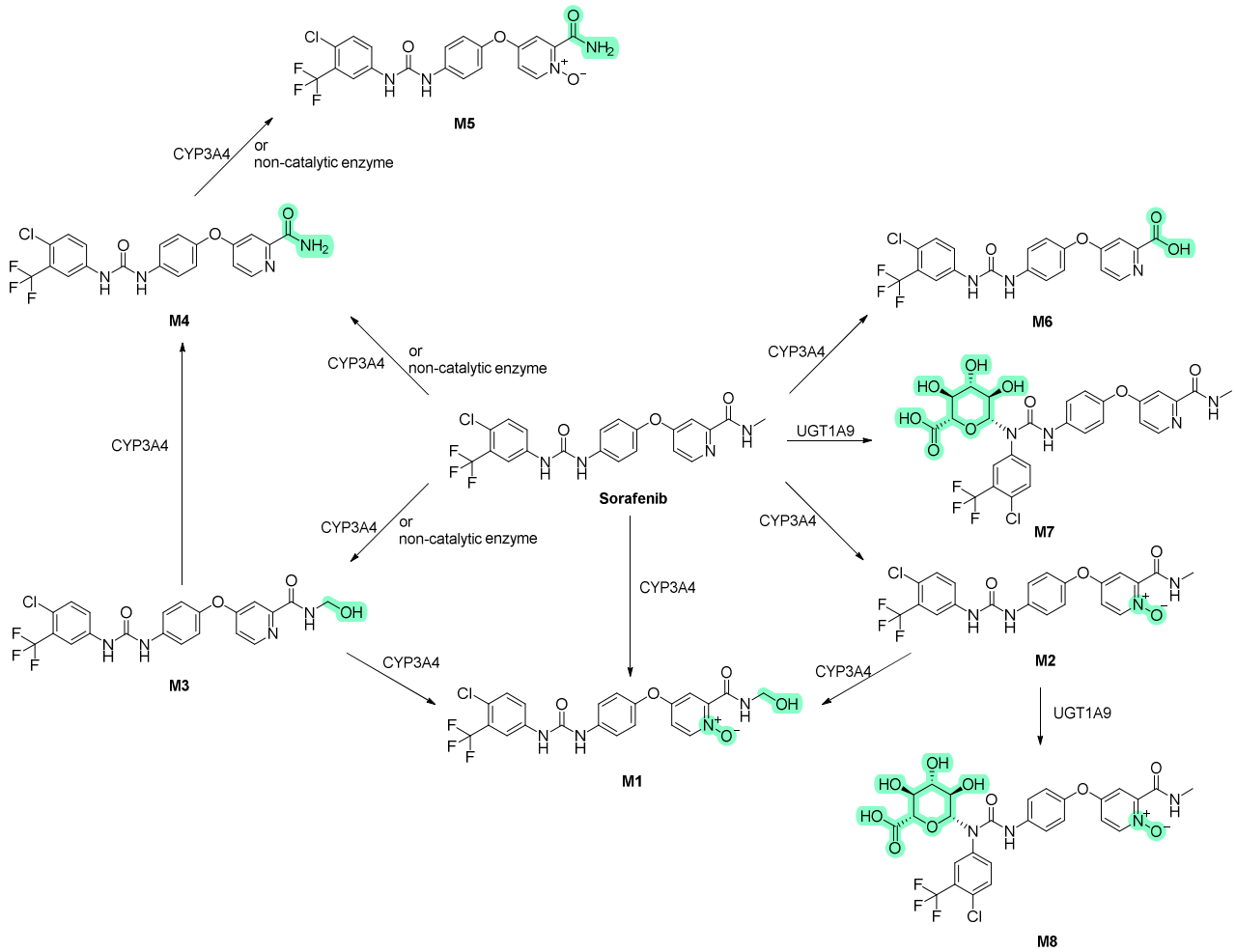

Fig. 1: Metabolism map of sorafenib and its metabolites.

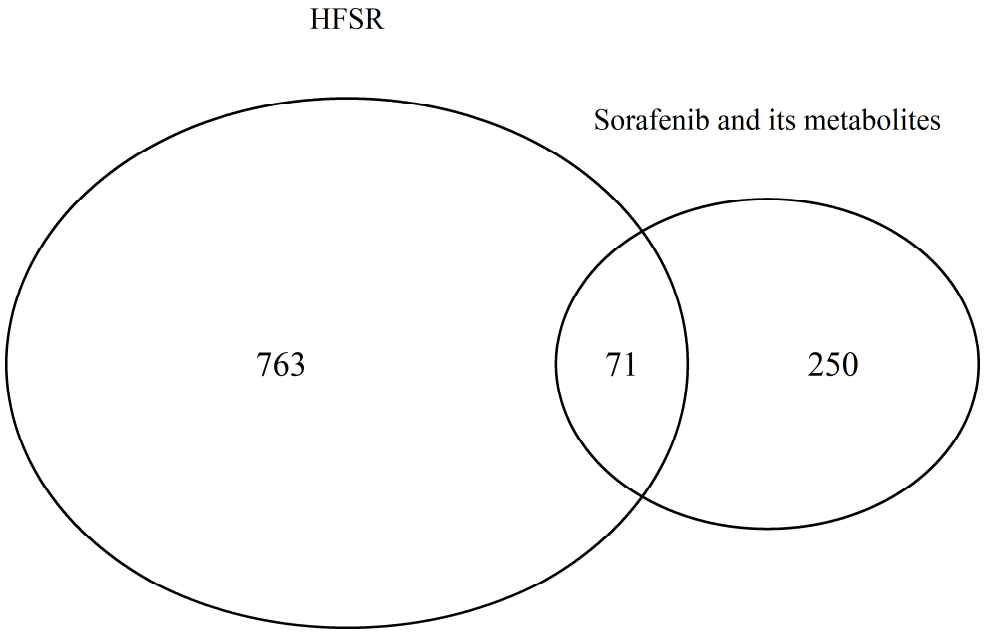

Fig. 2: Overlapping targets between sorafenib (and its metabolites) and HFSR-related targets.

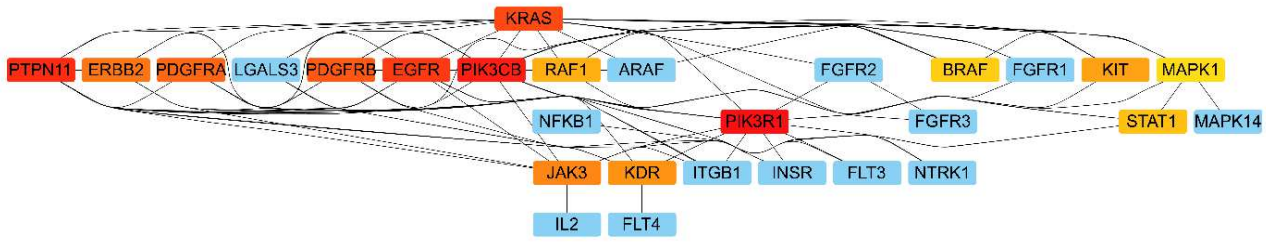

Fig. 3: PPI network of the 71 overlapping targets.

Table 1: Top 15 central hub genes ranked by MCC.

Rank	Display name	Score	Tissue::Skin
1	PIK3R1	1038	2.664916
2	PIK3CB	1036	3.630261
3	PTPN11	1030	3.161275
4	EGFR	982	3.728087
5	KRAS	896	3.173103
6	PDGFRB	744	3.1422
7	PDGFRA	726	2.989698
8	ERBB2	240	3.632999
9	JAK3	127	2.343779
10	KDR	26	2.881478
11	KIT	24	3.506328
12	RAF1	19	4.117622
13	STAT1	15	4.237799
14	BRAF	12	3.494023
15	MAPK1	11	3.552505

The resulting protein–protein interaction (PPI) network consisted of 70 nodes and 98 edges, exhibiting an average node degree of 2.8 and a clustering coefficient of 0.394 (Fig. 3). Hub genes were identified via topological analysis using the cytoHubba plugin in Cytoscape (v3.10.4). The top 15 nodes, ranked by Maximal Clique Centrality (MCC), were designated as the central hub genes (Table 1).

Functional enrichment analysis

As shown in Fig. 4, Metascape enrichment analysis of the top 15 hub genes (skin expression > 3.0 $\log_2$ (TPM + 1)) revealed a highly significant convergence on receptor tyrosine kinase (RTK) signaling pathways and their downstream cascades. The most enriched biological processes included cell surface receptor protein tyrosine kinase signaling, enzyme-linked receptor protein signaling, regulation of the MAPK cascade and the ERBB signaling pathway, alongside cell population proliferation and positive regulation of protein phosphorylation. At the cellular component level, receptor complexes, focal adhesions and cell-substrate junctions were prominently featured. Molecular function analysis highlighted protein kinase activity, transmembrane receptor protein tyrosine kinase activity and growth factor binding.

KEGG pathway analysis further underscored the involvement of central carbon metabolism in cancer, pancreatic cancer, EGFR tyrosine kinase inhibitor resistance and multiple cancer-specific pathways (prostate, endometrial, breast, melanoma and non-small cell lung cancer). Canonical pathways from PID showed strong enrichment in PDGFRB, ERBB1 proximal and downstream signaling, ERBB2/ERBB3 and SHP2 pathways. WikiPathways and Reactome analyses reinforced these findings, with significant hits in glioblastoma signaling, EGF/EGFR signaling, Ras and MAPK family cascades and aberrant PI3K/AKT signaling in cancer.

Compound–target–pathway network analysis

Compound–target–pathway network analysis revealed that sorafenib and its metabolites (M1–M8) converge on 8 core RTK-MAPK/PI3K nodes (EGFR, ERBB2, KIT, KRAS, PDGFRB, PIK3CB, MAPK1, RAF1). The most significant pathway enrichments were observed in Central Carbon Metabolism in Cancer (-log(q) = 15.09), Pancreatic Cancer (-log(q) = 14.98) and EGFR Tyrosine Kinase Inhibitor Resistance (-log(q) = 14.92). sorafenib and the metabolite M1 exhibit the broadest and fully overlapping target profiles, while M2–M3 act synergistically and M4–M8 partially overlap, collectively amplifying the off-target effects. The Sankey diagram (Fig. 5) illustrates Sorafenib's dominant flow through the EGFR–RAF1–MAPK1 axis to resistance pathways. The bubble plot (Fig. 6), using bubble size to represent gene count and color intensity for -$\log_{10}$(q-value), confirms that inhibition of the EGFR/RAF1-MAPK axis disrupts keratinocyte signaling and metabolism.

Molecular docking of sorafenib with potential targets

Molecular docking analysis focused on the key targets on the core RTK-MAPK/PI3K axis identified by network pharmacology: EGFR and ERK2 (MAPK1). Crystal structures co-crystallized with known inhibitors (EGFR–Sevabertinib, PDB: 9QXN; ERK2–AZD0364, PDB: 6SLG) were employed for the docking study. As shown in Fig. 7, sorafenib formed four conventional hydrogen bonds with residues LYS745, ASP800 and ASP855 in EGFR, with the optimal conformation exhibiting a –CDOCKER interaction energy of 48.6402 kcal/mol. As illustrated in Fig. 8, sorafenib also formed four conventional hydrogen bonds with residues LYS54, MET108, ASP111 and SER153 in ERK2, with the optimal conformation showing a –CDOCKER interaction energy of 52.6134 kcal/mol.

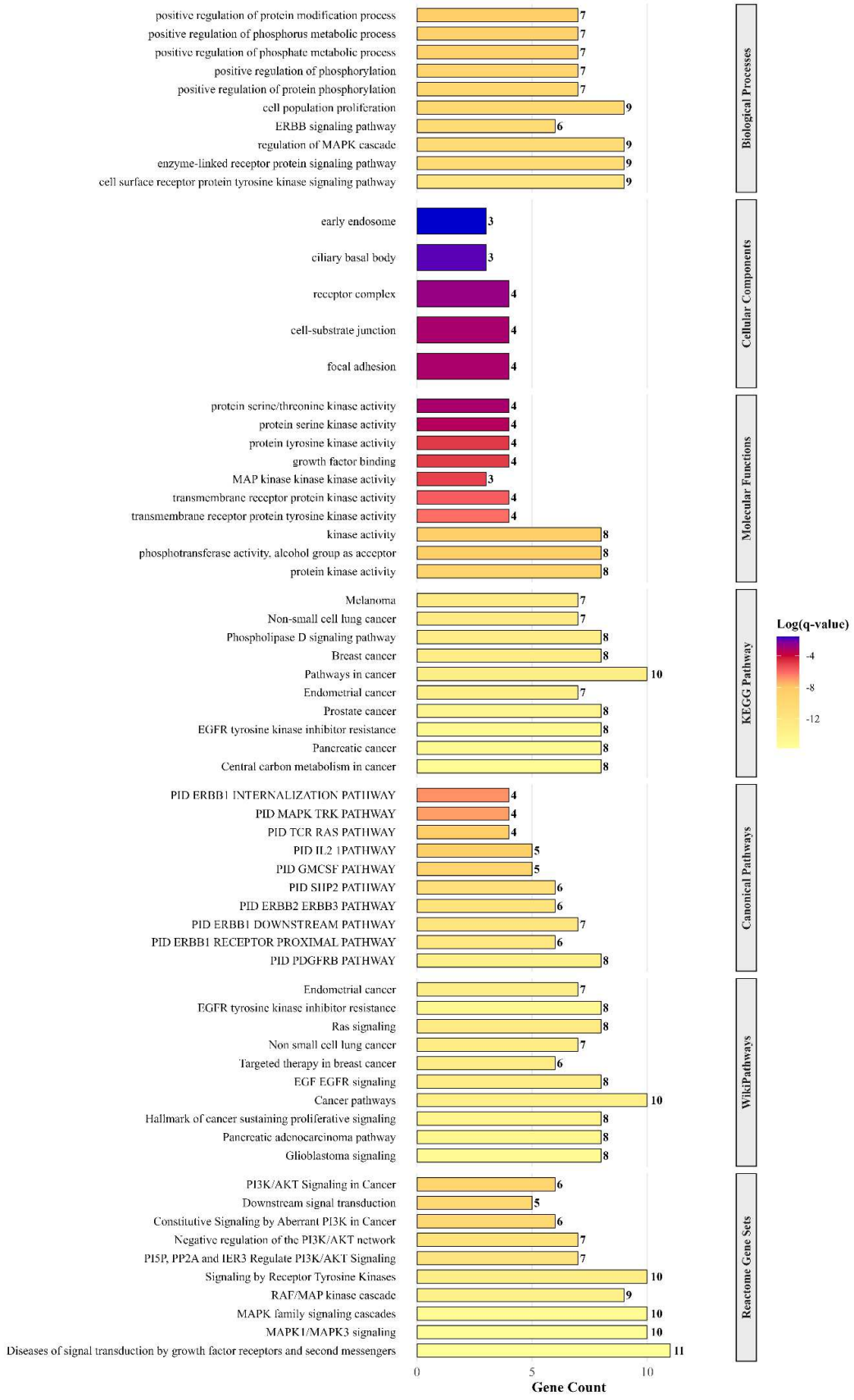

Fig. 4: Enrichment analysis of skin-highly expressed hub genes in sorafenib-induced HFSR.

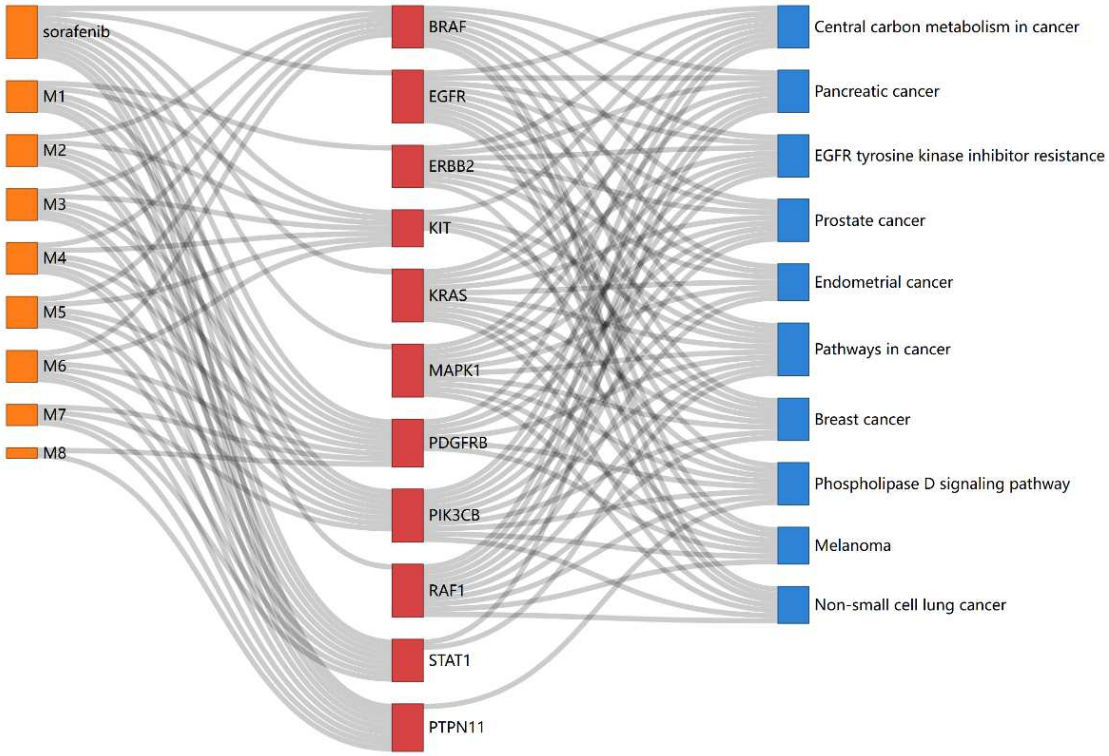

Fig. 5: Sankey diagram of compound-target-pathway network in sorafenib-induced HFSR.

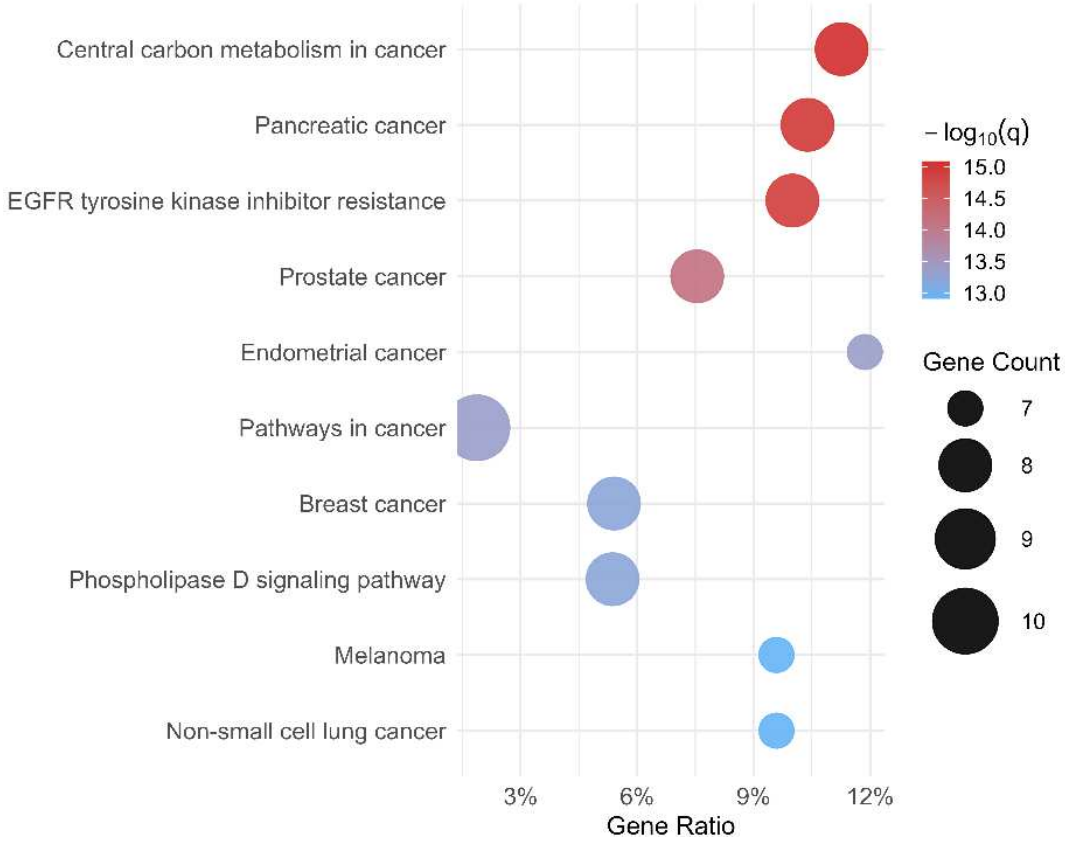

Fig. 6: Bubble plot of KEGG pathway enrichment.

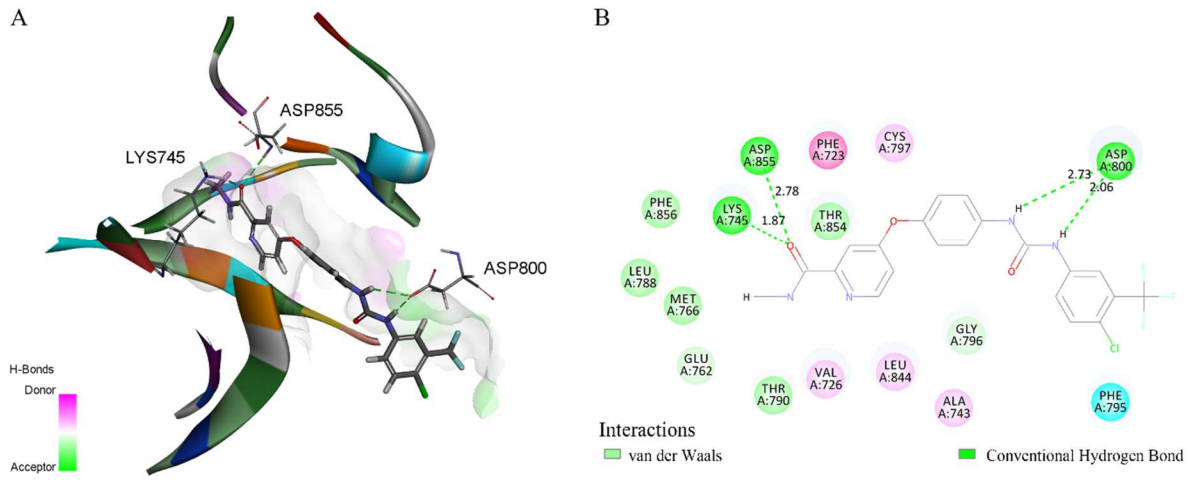

Fig. 7: Molecular docking of sorafenib with EGFR. (A) 3D binding conformation; (B) 2D interaction diagram at the binding site.

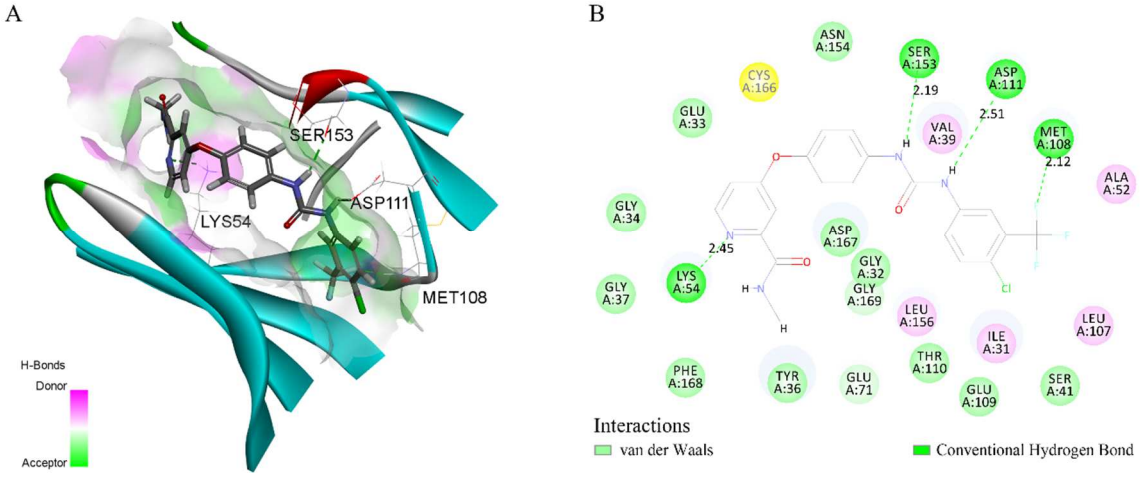

Fig. 8: Molecular docking of sorafenib with ERK2. (A) 3D binding conformation; (B) 2D interaction diagram at the binding site.

Molecular dynamics simulation results

Backbone-fitted ligand RMSD: The backbone-fitted ligand Root Mean Square Deviation (RMSD) profiles revealed distinct stabilization behaviors between the two complexes (Fig. 9). For the 9QXN–sorafenib system, the trajectory reached a stable plateau after approximately 18.45 ns, with a stable-phase RMSD of 0.199 ± 0.050 nm. In contrast, the 6SLG–Sorafenib complex stabilized earlier, at 5.5 ns, but exhibited a slightly higher RMSD of 0.236 ± 0.040 nm during the equilibrium phase.

Binding pocket residue flexibility (RMSF): Analysis of Root Mean Square Fluctuation (RMSF) for binding-site residues (≤0.5 nm) demonstrated lower overall flexibility in 9QXN compared with 6SLG (mean RMSF 0.0938 nm vs. 0.129 nm, respectively) (Fig. 10). The most fluctuating residues in 6SLG (e.g., 36, 114, 56) reached RMSF values up to 0.324 nm, whereas the highest fluctuation in 9QXN was 0.289 nm at residue 723.

Distance between ligand COM and pocket COM: The center-of-mass (COM) distance analysis revealed markedly different ligand retention behaviors (Fig. 11). In the 9QXN–Sorafenib system, the COM distance remained tightly clustered at 2.50 ± 0.28 nm, with a minimal range (1.64–5.13 nm), indicative of persistent anchoring within the binding cavity. Conversely, the 6SLG complex displayed a wider distribution (8.24 ± 0.85 nm, range 5.47–12.0 nm).

Hydrogen bond analysis: Hydrogen bond analysis further supported the difference in binding stability (Fig. 12). The 9QXN–Sorafenib complex maintained 0.90 ± 0.62 hydrogen bonds on average (max 4), whereas the 6SLG system formed only 0.39 ± 0.70 hydrogen bonds (max 5). The low mean value in 6SLG, despite transient peaks, indicates sporadic and unstable hydrogen-bonding interactions, while 9QXN consistently maintained at least one hydrogen bond throughout the stable phase.

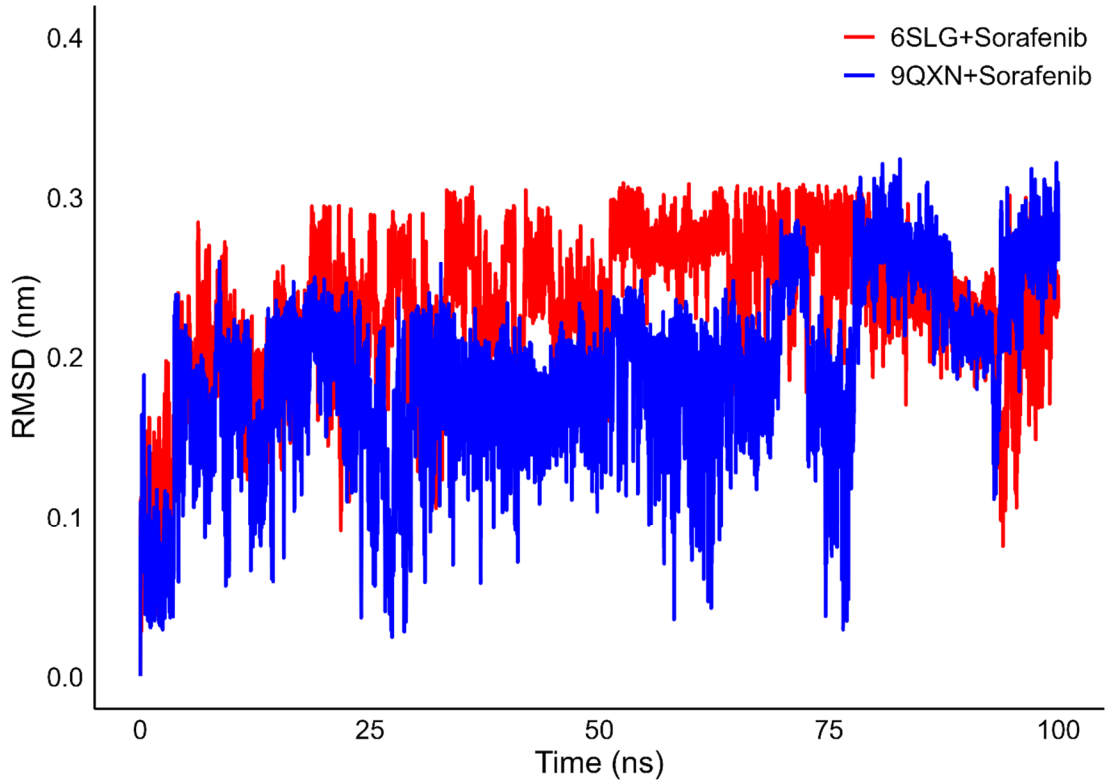

Fig. 9: Backbone-fitted ligand RMSD profiles of the sorafenib–protein complexes.

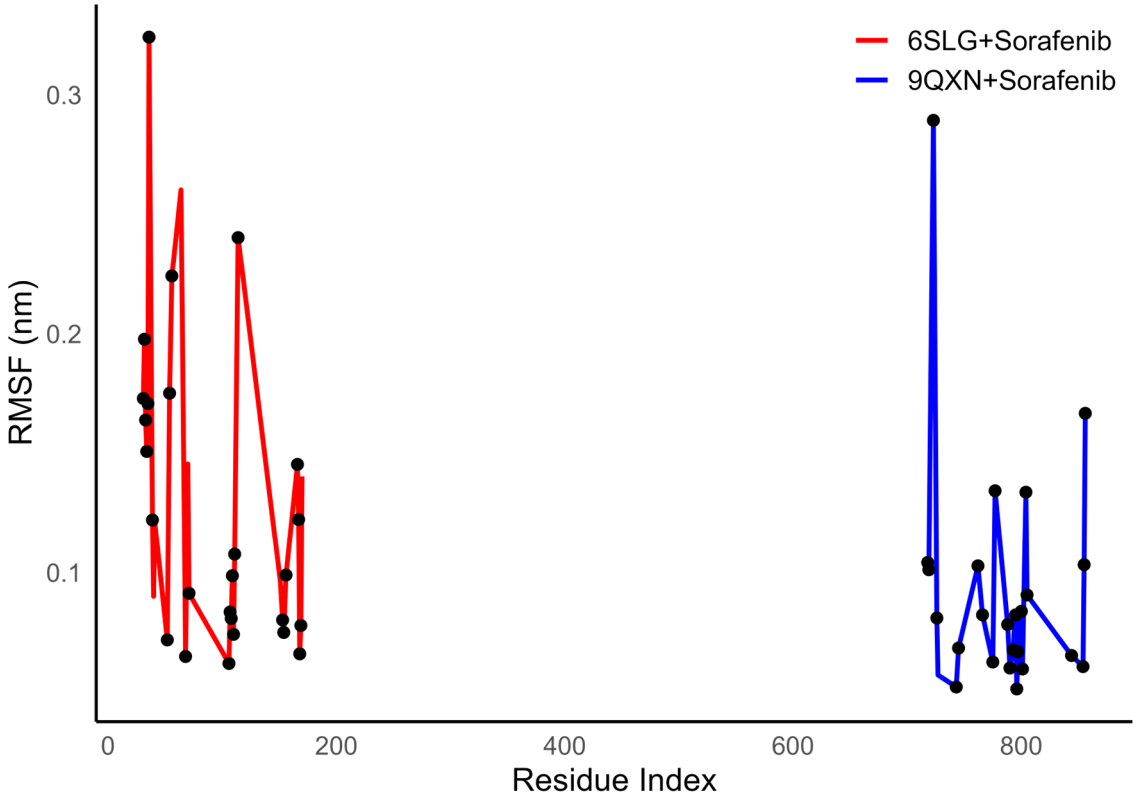

Fig. 10: RMSF values of binding-site residues in the sorafenib–protein complexes.

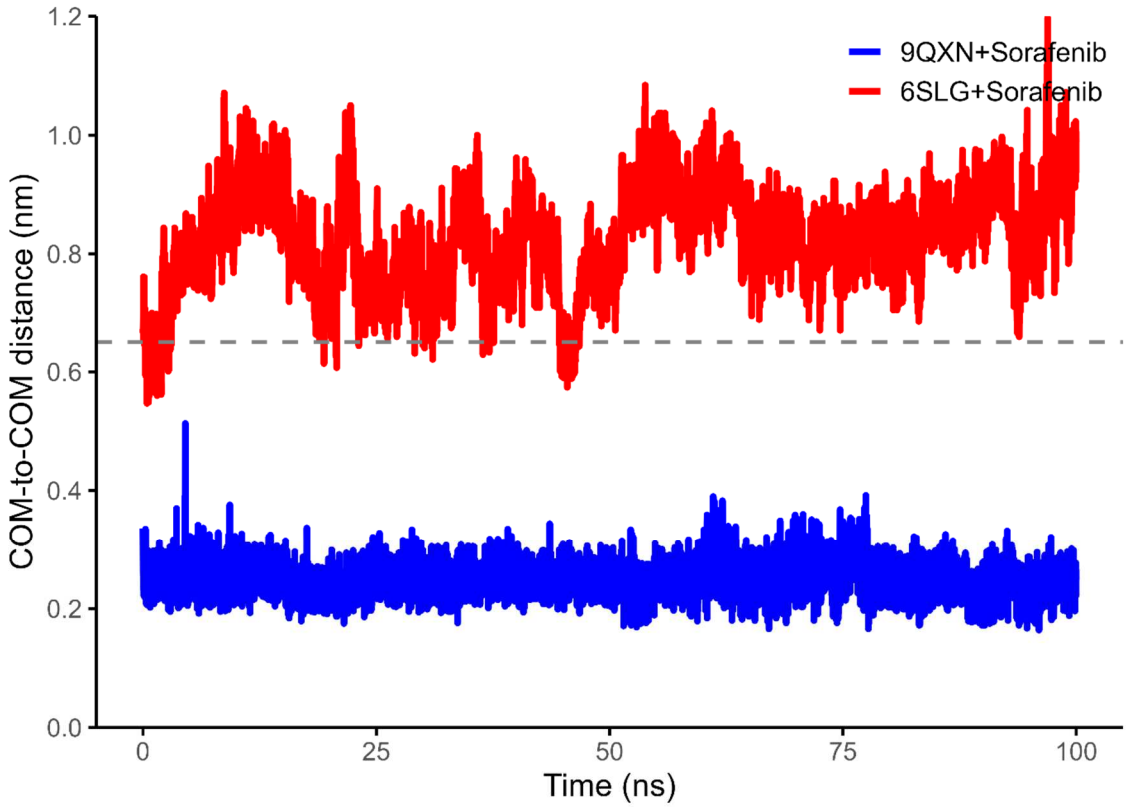

Fig. 11: Time-evolution of the COM distance between sorafenib and the binding pocket.

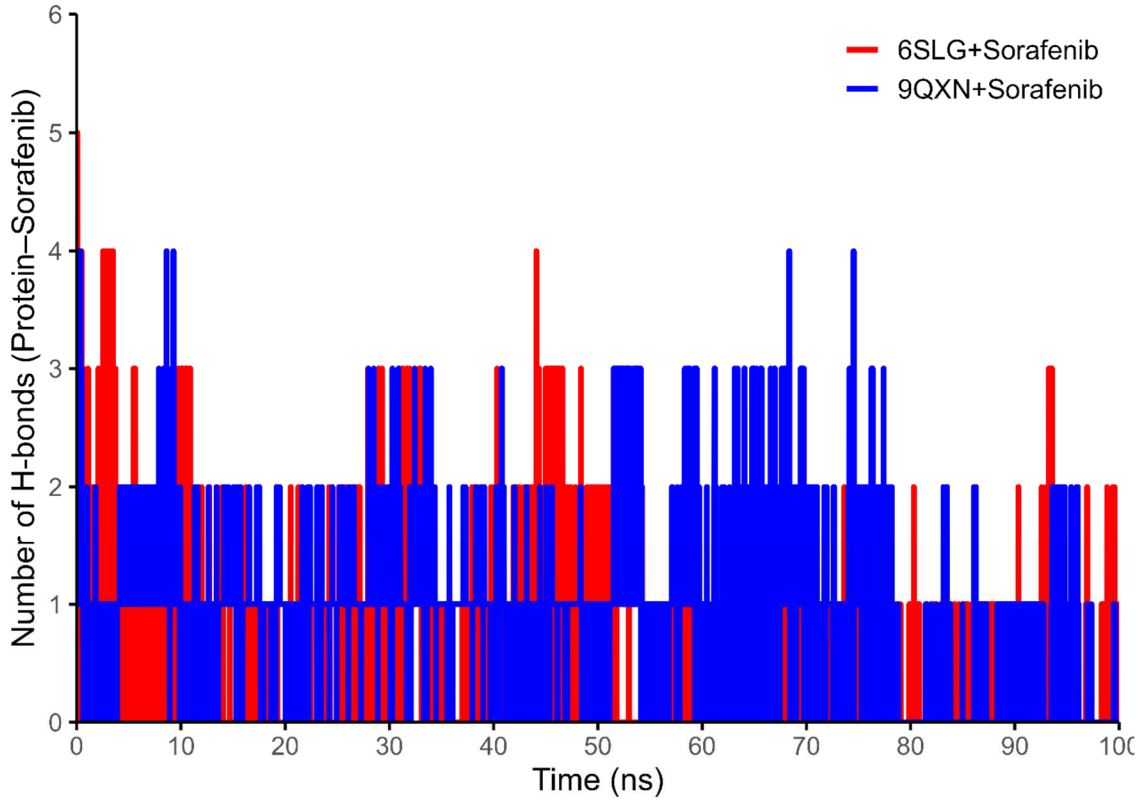

Fig. 12: Time-dependent changes in the hydrogen bonds formed between sorafenib and proteins.

DISCUSSION

The compound–target–pathway network analysis further refined this mechanism, showing that sorafenib and its metabolites converge on 8 core RTK-MAPK/PI3K nodes, specifically involving EGFR, MAPK1 (ERK2) and RAF1. This convergence suggests that cutaneous toxicity is mediated by the accumulation of multiple off-target effects rather than a single event (Chen *et al*., 2022, Liang *et al*., 2025, Moon *et al*., 2021, Siddharth *et al*., 2022, Takao *et al*., 2022, Wang *et al*., 2021).

The biological relevance of these core targets is strongly supported by recent literature. Our findings resonate with the recent work showing that epiregulin drives keratinocyte hyperproliferation through EGFR signaling, identified as a key pathological mechanism of HFSR (Liang *et al*., 2025). Consequently, off-target inhibition or dysregulation of EGFR by sorafenib may directly impair skin homeostasis and repair. MAPK1 (ERK2), as a downstream effector of the MAPK cascade, has a central role in regulating keratinocyte proliferation, differentiation and wound repair (Satoh *et al*., 2009); its functional disruption is closely implicated in HFSR pathology. Furthermore, RAF1 inhibition, sorafenib's primary mechanism, can trigger complex feedback mechanisms, potentially impacting skin cells through paradoxical activation or alteration of downstream ERK/MAPK activity (Wei *et al*., 2025).

Crucially, these computational predictions are strongly supported by existing biological and clinical evidence: histopathological examinations of HFSR lesions revealing epidermal hyperkeratosis and keratinocyte ballooning (Yang *et al*., 2008) are highly consistent with the known effects of EGFR- and MAPK-related dysregulation on keratinocyte proliferation and differentiation. In parallel, pharmacokinetic analyses confirm that sorafenib and its metabolites reach measurable local concentrations in human skin (Hussaarts *et al*., 2020), providing the necessary basis for these local off-target effects.

To validate the off-target hypothesis at the molecular level, we focused on the most critical components. Given the trace amounts and minimal systemic exposure of the metabolite M1 (Gong *et al*., 2017), sorafenib was selected as the dominant active entity for the simulation studies. Due to structural uncertainties regarding RAF1, molecular docking and dynamics simulations were strategically concentrated on the two structurally validated targets, EGFR and ERK2. Initial docking results confirmed favorable binding energies and stable hydrogen bonds for sorafenib with both targets, preliminarily supporting their potential for off-target engagement.

However, the subsequent molecular dynamics simulations provided the key mechanistic insight. The collective results from all dynamic metrics (RMSD, RMSF, COM distance and hydrogen bond analysis) consistently demonstrated that the sorafenib–EGFR (PDB: 9QXN) complex exhibits significantly superior dynamic binding stability compared to the sorafenib–ERK2 (PDB: 6SLG) complex. While the static molecular docking affinity was slightly higher for ERK2 (52.6134 kcal/mol), the dynamic simulation revealed that sorafenib adopts a more rigid, persistent and tightly anchored binding mode within the EGFR pocket. This finding suggests that, in the physiological skin environment, sorafenib may exhibit higher binding persistence and greater pharmacological relevance for the EGFR target, which is crucial for explaining the mechanism of its off-target cutaneous toxicity.

In summary, this study provides a coherent mechanistic hypothesis: sorafenib and its metabolites induce HFSR through the accumulated dysregulation of RTK–MAPK/PI3K signaling in skin tissues, leading to altered keratinocyte proliferation, adhesion and inflammatory responses (Chen *et al*., 2020, Gong *et al*., 2017, Morgos *et al*., 2024, Stefani *et al*., 2021, Üremiş *et al*., 2023). A key limitation remains the reliance on public disease–gene associations lacking phenotype specificity. Future experimental validation of the mediating roles of the EGFR and ERK2 pathways in skin models is essential to confirm these computational hypotheses.

CONCLUSION

This study successfully employed a computational pharmacology approach to delineate the molecular mechanism underlying sorafenib-induced Hand–Foot Skin Reaction (HFSR). Our network analysis strongly linked HFSR pathogenesis to the abnormal activation of the RTK-MAPK/ERK and PI3K-Akt signaling pathways, identifying EGFR and ERK2 as central toxicological targets. Molecular dynamics simulations further suggested that sorafenib's off-target interference with both of these critical pathways collectively drives the pathological process in skin keratinocytes. The plausibility of these computational predictions is reinforced by recent literature: for instance, *in-vitro* studies have confirmed that the upregulation of the EGFR ligand epiregulin (EREG) drives keratinocyte hyperproliferation in HFSR(Liang *et al*., 2025), while reviews underscore the central role of the RTK-MAPK/PI3K axis in sorafenib-associated toxicity(Abizadeh *et al*., 2025). These findings provide an important predictive mechanistic framework for understanding Sorafenib-related cutaneous toxicity.

It is crucial to state that all conclusions drawn in this study are based entirely on pure computational models, which constitutes the primary limitation of our work. Future efforts must focus on experimental validation, involving *in vitro* cell models or protein activity analysis in clinical samples, to confirm the mediating roles of the EGFR and ERK2 pathways. This validation is essential to translate our

computational hypotheses into reliable biological evidence, ultimately guiding the development of prophylactic and therapeutic strategies for HFSR.

Acknowledgement
We gratefully acknowledge Li Yang of Bohai University for providing the Discovery Studio 2017 software and related technical support.

Authors' contributions
LQW and SQZ: Software usage, conceptualization, methodology, writing—original draft; LG and JQL: Data curation, formal analysis; LHL: Analysis, interpretation; GZZ: Supervision, funding acquisition, writing—review and editing.

Funding
This research was funded by the Jinzhou Medical University Undergraduate Innovation and Entrepreneurship Training Program (grant number X202410160078) and the Liaoning Provincial Science and Technology Joint Program (Natural Science Foundation – General Project, Grant No. 2025-MSLH-238).

Data availability statement
The datasets generated and analysed during the current study are available from the corresponding author on reasonable request.

Ethical approval
Not applicable.

Conflict of interest
The authors declare no conflict of interest.

REFERENCES

Abizadeh E, Berglas E, Abizadeh A, Glatman J, Lavi AB, Spivak M, Sapir T and Shifteh D (2025). Current and emerging therapies for targeting the ERK1/2 and PI3K pathways in cancer. *Int. J. Mol. Sci.*, **26**(17): 8696.

Adefisan-Adeoye AO, Odewale MO and Adaramoye OA (2025). Haematological and biochemical changes in sorafenib-induced renal toxicity. *Saudi J Med*, **10**(9): 464-473.

Ahmad Roslan NSB, Roney M, Issahaku AR, Uddin MN, Mohd Aluwi MFF, Zareen S, Wilhelm A, Gazali AM, Akhtar MN. Zamri NB (2025). Unveiling the potential of garcinia atroviridis root-derived phenolic compounds against breast cancer: Isolation, network pharmacology and in-silico approaches. *J. Pharm. Innov.*, **20**(6): 1-17.

Baby B, Sam N, MP N, Anjaneyan G and MP R (2025). Therapy-related hand-foot syndrome: A review. *J. Chemother.*, **37**(7): 567-578.

Balasundaram A, Kumar SU and Doss CGP (2022). A computational model revealing the immune-related hub genes and key pathways involved in rheumatoid arthritis (RA). *Adv. Protein Chem. Struct. Biol.*, **129**: 247-273.

Cai H, Du X, Deng Y, Cao D, Wang L, Wu Z, Zhang X, Xu J and Xie B (2024). Pharmacokinetics and apparent Michaelis constant for metabolite conversion of sorafenib in healthy and hepatocellular carcinoma-bearing rats. *Bioanalysis*, **16**(10): 461-473.

Chen CT, Liao LZ, Lu CH, Huang YH, Lin YK, Lin JH and Chow LP (2020). Quantitative phosphoproteomic analysis identifies the potential therapeutic target EphA2 for overcoming sorafenib resistance in hepatocellular carcinoma cells. *Exp. Mol. Med.*, **52**(3): 497-513.

Chen C, Wu Y, Li J, Wang X, Zeng Z, Xu J, Liu Y, Feng J, Chen H and He Y (2023). TBtools-II: A "one for all, all for one" bioinformatics platform for biological big-data mining. *Molecular plant*, **16**(11): 1733-1742.

Chen J and Wang Z (2021). How to conduct integrated pharmaceutical care for patients with hand-foot syndrome associated with chemotherapeutic agents and targeted drugs. *J. Oncol. Pharm. Pract.*, **27**(4): 919-929.

Chen L, Wu Z, Yang L, Chen Y, Wang W, Cheng L, Li C, Lv D, Xia L and Chen J (2022). Nitric oxide in multikinase inhibitor-induced hand–foot skin reaction. *Translational Research*, **245**: 82-98.

Franczyk B, Rysz J and Gluba-Brzozka A (2022). Pharmacogenetics of drugs used in the treatment of cancers. *Genes*, **13**(2): 311.

Gong L, Giacomini MM, Giacomini C, Maitland ML, Altman RB. Klein TE (2017). PharmGKB summary: sorafenib pathways. *Pharmacogenet. Genomics*, **27**(6): 240-246.

Guo L, Hu C, Yao M and Han G (2023). Mechanism of sorafenib resistance associated with ferroptosis in HCC. *Front. Pharmacol.*, **14**: 1207496.

Hussaarts KG, van Doorn L, Eechoute K, Damman J, Fu Q, van Doorn N, Eisenmann ED, Gibson AA, Oomen-de Hoop E and de Bruijn P (2020). Influence of probenecid on the pharmacokinetics and pharmacodynamics of sorafenib. *Pharmaceutics*, **12**(9): 788.

Inaba H, Panetta JC, Pounds SB, Wang L, Li L, Navid F, Federico SM, Eisenmann ED, Vasilyeva A and Wang YD (2019). Sorafenib population pharmacokinetics and skin toxicities in children and adolescents with refractory/relapsed leukemia or solid tumor malignancies. *Clinical Cancer Research*, **25**(24): 7320-7330.

Kumar N, Mishra B and Mukhtar MS (2022). A pipeline of integrating transcriptome and interactome to elucidate central nodes in host-pathogens interactions. *STAR protocols*, **3**(3): 101608.

Kumari YA, Gulabi S, Sushma A and Sindhu MS (2022). Hand foot skin reaction with multikinase inhibitor sorafenib-A rare case report. *J. YSR Univ. Health Sci.,* **11**(4): 369-372.

Lee Y-S, Jung YK, Kim JH, Cho SB, Kim DY, Kim MY,

Kim HJ, Seo YS, Yoon KT and Hong YM (2020). Effect of urea cream on sorafenib-associated hand–foot skin reaction in patients with hepatocellular carcinoma: A multicenter, randomised, double-blind controlled study. *Eur. J. Cancer*, **140**: 19-27.

Li J, Zhang L, Ge T, Liu J, Wang C and Yu Q (2024). Understanding sorafenib-induced cardiovascular toxicity: Mechanisms and treatment implications. *Drug Des. Devel. Ther.*, 829-843.

Liang F, Zhang K, Ma W, Zhan H, Sun Q, Xie L and Zhao Z (2022). Impaired autophagy and mitochondrial dynamics are involved in Sorafenib-induced cardiomyocyte apoptosis. *Toxicology*, **481**: 153348.

Liang Y, Hong X, Zhong X, Chen K, Wang J, Zhao J, Li Z, Wu J, Zhou G and Huang X (2025). Epiregulin drives keratinocyte hyperproliferation in sorafenib-induced hand-foot skin reaction: A mechanistic and therapeutic insight. *Clinics*, **80**: 100809.

Lim C, Lee D, Kim M, Lee S, Shin Y, Ramsey JD, Choi H-G, Lee ES, Youn YS and Oh KT (2023). Development of a sorafenib-loaded solid self-nanoemulsifying drug delivery system: Formulation optimization and characterization of enhanced properties. *J. Drug Deliv. Sci. Technol.*, **82**: 104374.

Liu ZL, Chen HH, Zheng LL, Sun LP and Shi L (2023). Angiogenic signaling pathways and anti-angiogenic therapy for cancer. *Signal transduction and targeted therapy*, **8**(1): 198.

Moon H and Ro SW (2021). MAPK/ERK signaling pathway in hepatocellular carcinoma. *Cancers (Basel)*, **13**(12): 3026.

Morgos DT, Stefani C, Miricescu D, Greabu M, Stanciu S, Nica S, Stanescu-Spinu II, Balan DG, Balcangiu-Stroescu AE and Coculescu EC (2024). Targeting PI3K/AKT/mTOR and MAPK signaling pathways in gastric cancer. *Int. J. Mol. Sci.*, **25**(3): 1848.

Ochi M, Kamoshida T, Araki M and Ikegami T (2021). Prolonged survival in patients with hand–foot skin reaction secondary to cooperative sorafenib treatment. *World J. Gastroenterol.*, **27**(32): 5424.

Panetta JC, Campagne O, Gartrell J, Furman W and Stewart CF (2021). Pharmacokinetically guided dosing of oral sorafenib in pediatric hepatocellular carcinoma: A simulation study. *Clin. Transl. Sci.*, **14**(6): 2152-2160.

Pang Y, Eresen A, Zhang Z, Hou Q, Wang Y, Yaghmai V and Zhang Z (2022). Adverse events of sorafenib in hepatocellular carcinoma treatment. *Am. J. Cancer Res.*, **12**(6): 2770.

Piñero J, Ramirez-Anguita JM, Sauch-Pitarch J, Ronzano F, Centeno E, Sanz F and Furlong LI (2020). The DisGeNET knowledge platform for disease genomics: 2019 update. *Nucleic Acids Res.*, **48**(D1): D845-D855.

Qin Y, Han S, Yu Y, Qi D, Ran M, Yang M, Liu Y, Li Y, Lu L and Liu Y (2024). Lenvatinib in hepatocellular carcinoma: Resistance mechanisms and strategies for improved efficacy. *Liver International*, **44**(8): 1808-1831.

Raju SK, Sekar P, Sundhararajan N, Alotaibi BS, Sankarganesh M, Bhat AR and Ahmed S (2025). Theoretical, *in-vitro* antiproliferative and *in-silico* molecular docking and pharmacokinetics studies of dehydrozingerone mannich base heterocyclic derivatives. *J. Biochem. Mol. Toxicol.,* **39**(12): e70650.

Rui K, Kamata Y, Tominaga M, Kishi R, Kaneko T, Tsujimura A, Yasushi S and Takamori K (2025). Possible clinical effects of ketoconazole on sorafenib-induced hand–foot skin reaction and cytoprotection mechanisms of antifungal agents against multikinase inhibitor-induced keratinocyte Toxicity. *Acta Derm. Venereol.*, **105**: 40697.

Saigusa D, Matsukawa N, Hishinuma E and Koshiba S (2021). Identification of biomarkers to diagnose diseases and find adverse drug reactions by metabolomics. *Drug Metab. Pharmacokinet.*, **37**: 100373.

Satoh Y, Saitoh D, Takeuchi A, Ojima K, Kouzu K, Kawakami S, Ito M, Ishihara M, Sato S and Takishima K (2009). ERK2 dependent signaling contributes to wound healing after a partial-thickness burn. *Biochem. Biophys. Res. Commun.*, **381**(1): 118-122.

Siddharth S, Kuppusamy P, Wu Q, Nagalingam A, Saxena NK and Sharma D (2022). Metformin enhances the anti-cancer efficacy of sorafenib via suppressing MAPK/ERK/Stat3 axis in hepatocellular carcinoma. *Int. J. Mol. Sci.*, **23**(15): 8083.

Song S, Huang L, Zhou X and Yu J (2025). Exploring the toxicological network in diabetic microvascular disease. *Int. J. Surg.*, **111**(6): 3895-3907.

Stefani C, Miricescu D, Stanescu-Spinu I-I, Nica RI, Greabu M, Totan AR and Jinga M (2021). Growth factors, PI3K/AKT/mTOR and MAPK signaling pathways in colorectal cancer pathogenesis: Where are we now? *Int. J. Mol. Sci.*, **22**(19): 10260.

Stelzer G, Rosen N, Plaschkes I, Zimmerman S, Twik M, Fishilevich S, Stein TI, Nudel R, Lieder I and Mazor Y (2016). The GeneCards suite: From gene data mining to disease genome sequence analyses. *Curr. Protoc. Bioinf.*, **54**(1): 1.30. 31-31.30. 33.

Szklarczyk D, Nastou K, Koutrouli M, Kirsch R, Mehryary F, Hachilif R, Hu D, Peluso ME, Huang Q and Fang T (2025). The STRING database in 2025: protein networks with directionality of regulation. *Nucleic Acids Res.*, **53**(D1): D730-D737.

Takao T, Masuda H, Kajitani T, Miki F, Miyazaki K, Yoshimasa Y, Katakura S, Tomisato S, Uchida S and Uchida H (2022). Sorafenib targets and inhibits the oncogenic properties of endometrial cancer stem cells via the RAF/ERK pathway. *Stem Cell. Res. Ther.*, **13**(1): 225.

Trivedi M, Mehta RD, Ghiya BC and Soni P (2023). Sorafenib-induced hand–foot skin reaction. *J. Radiat. Cancer Res.,* **14**(3): 160-161.

Uremis MM, Uremis N and Turkoz Y (2023). Cucurbitacin E shows synergistic effect with sorafenib by inducing

apoptosis in hepatocellular carcinoma cells and regulates Jak/Stat3, ERK/MAPK, PI3K/Akt/mTOR signaling pathways. *Steroids*, **198**: 109261.

Wang F, Zhang X, Wang Y, Chen Y, Lu H, Meng X, Ye X and Chen W (2023). Activation/inactivation of anticancer drugs by CYP3A4: Influencing factors for personalized cancer therapy. *Drug Metab. Disposition*, **51**(5): 543-559.

Wang LT, Liu KY, Chiou SS, Huang SK, Hsu SH and Wang SN (2021). Phosphorylation of intestine-specific homeobox by ERK1 modulates oncogenic activity and sorafenib resistance. *Cancer Lett.*, **520**: 160-171.

Wang W, Chen F, Hu Y, Sun D, Chang J, Lin L and Ding H (2025). Mechanism study of naringenin in treating sepsis-induced kidney injury based on network pharmacology. *Pak. J. Pharm. Sci.*, **38**(2): 373-379.

Wei M, Cao Z, Dong L, Wang W, Wei M, Ji L, Duan L, Sun H and Zheng M (2025). The advantages and challenges of sorafenib combination therapy: Drug resistance, toxicity and future directions. *Oncol. Lett.*, **30**(5): 526.

Wieczór M, Czub J and Orozco M (2025). Gromologist: a gromacs-oriented utility library for structure and topology manipulation. *SoftwareX*, **30**: 102118.

Yang CH, Lin WC, Chuang CK, Chang YC, Pang ST, Lin YC, Kuo TT, Hsieh JJ and Chang J (2008). Hand–foot skin reaction in patients treated with sorafenib: A clinicopathological study of cutaneous manifestations due to multitargeted kinase inhibitor therapy. *Br. J. Dermatol.*, **158**(3): 592-596.

Zaru R, Orchard S and Consortium U (2023). UniProt tools: BLAST, align, peptide search and ID mapping. *Current protocols*, **3**(3): e697.

Zhang D, Cai Y, Sun Y, Zeng P, Wang W, Wang W, Jiang X and Lian Y (2024). A real-world pharmacovigilance study of Sorafenib based on the FDA adverse event reporting system. *Front. Pharmacol.*, **15**: 1442765.